NOTES AND CORRESPONDENCE

Conditions Associated with Large-Drop Regions

BRENDA M. POBANZ AND JOHN D. MARWITZ

Department of Atmospheric Science, University of Wyoming, Laramie, Wyoming

MARCIA K. POLITOVICH

Research Applications Program, National Center for Atmospheric Research, Boulder, Colorado

1 September 1992 and 4 March 1994

ABSTRACT

In light of the significant icing hazard large drops pose to general aviation, two conditions have been previously associated with large-drop formation; these being a warm cloud-top temperature and a low droplet concentration. This paper identifies an additional condition associated with the development of large-drop regions. Wind shear is hypothesized as being a necessary but not sufficient condition for the formation of large drops. Wind shear at cloud top may cause turbulence, Kelvin–Helmholtz waves, and thus the inhomogeneous mixing leading to large drops.

This hypothesis was tested in 29 cases where the Wyoming King Air aircraft made a climb or descent through the top of stratiform clouds. The presence of a wind shear layer was defined by the magnitude of the wind shear and the value of the bulk Richardson number across the layer. In 23 of the 29 cases, wind shear was associated with large-drop regions. A χ^2 statistical test was applied to the data. The null hypothesis, where wind shear and large drops were considered independent of each other, was rejected to a significance level of 0.01. From this it can be inferred that large drops and wind shear are related. The depth of the shear layer was usually small, less than 150 m. The validity of the condition of low droplet concentration is questioned since several cases of large drops were found in the presence of a high droplet concentration. These cases were marked by strong wind shear.

1. Introduction

Icing caused by large supercooled drops can present a significant hazard to aviation. We define large-drop icing as that caused by drops of approximately 30–250-μm diameter. These large drops can flow along the airfoil prior to freezing, and may accrete on surfaces not guarded by deicing equipment. They generally form what is known as clear or glaze ice. Clear icing on the wings is particularly insidious, since the pilot may not become aware of its presence in time to take evasive action. A seemingly small amount of ice on the lower and upper surface of an airfoil has the potential for serious disruption of the airflow around a wing and may adversely increase the coefficient of drag and stall speed (Cooper et al. 1984).

Several cases of large-drop icing that occurred over the Sierra Nevada in California are described by Cooper et al. (1984) and Sand et al. (1984). Politovich (1989) examined these and additional encounters and summarized meteorological conditions accompanying the presence of large drops. These conditions were relatively warm cloud-top temperatures (CT > −15°C), weak thermodynamic instability, and low droplet concentrations.

Warm cloud tops are favored since they decrease the probability of ice initiation, which depletes cloud liquid through depositional growth and riming. Thermodynamic instability results in weak convective updrafts providing time and liquid water for hydrometeor growth in the cloud. In addition, weak thermodynamic instability tends to result in cloud-top entrainment and, hence, evaporation of cloud liquid. Low droplet concentrations were present in the examples presented by Politovich (1989) and are generally associated with maritime stratiform clouds due to their weak updrafts and low concentrations of cloud condensation nuclei. The fewer but larger droplets collide and coalesce more readily than smaller droplets.

To examine the effect of these conditions on coalescence growth, Song and Marwitz (1989) performed numerical simulations of stratiform clouds with warm tops and low droplet concentrations. The model microphysical processes included condensation, coales-

Corresponding author address: Prof. John D. Marwitz, Department of Atmospheric Science, University of Wyoming, P.O. Box 3038, Laramie, WY 82071.

cence, and sedimentation. Results indicated that the time required to grow drops with diameters 100–500 μm was on the order of hours. On the other hand, droplets have been observed to grow to this size in similar clouds on the order to tens of minutes. This implies that the conditions suggested by Politovich (1989) were not sufficient to explain the formation of large drops.

Obviously an additional condition is needed. In this paper we examine the hypothesis that dynamically unstable shear layers at the tops of stratiform clouds are related to large-drop regions. Wind shear at the top of a cloud in a thermodynamically stable atmosphere may cause a dynamically unstable layer and hence, turbulence and possibly Kelvin–Helmholtz (KH) waves, entrainment of subsaturated air, and mixing. This note will not address the issue of how mixing results in large drops, but will report on the observed conditions associated with such regions.

The field projects in which data on large drops were collected, the instrumentation onboard the aircraft, and the definitions of a large-drop region and a dynamically unstable shear layer are presented in section 2. The general results for 29 soundings through cloud tops, a specific case study, and the overall results are summarized in section 3. The results and implications are discussed in section 4.

2. Data

a. Field projects

The measurements used in this study were collected during two field projects: the Sierra Cooperative Pilot Project (SCPP, Reynolds and Dennis 1986) and the Winter Icing and Storms Project (WISP, Rasmussen et al. 1992).

Large drops were first encountered in SCPP during the fifth season, 1981/82. This prompted further study of large-drop regions during the remaining five seasons of SCPP and during WISP. Unfortunately, for the flights used in Politovich (1989), the aircraft did not routinely sample the cloud-top area nor the region above the cloud in the vicinity of the large-drop regions; thus, much information regarding the origins of the drops is lacking.

WISP was designed specifically to study the production and depletion of supercooled liquid water in winter storms. One area receiving special attention was that of large-drop formation. Flight plans were designed to specifically sample large-drop regions: ascents and descents were made through the entire depth of the cloud, and vertical sawtooth patterns were conducted through the upper 200 m of cloud. During WISP, several encounters with large-drop regions were recorded; these are included in the dataset discussed below.

b. Instrumentation

The instrumentation used for these studies is described by Cooper et al. (1984). Winds were measured using a Litton (LTN-51) Inertial Navigation System and a Rosemount (858AJ) deiced differential gust probe for wind calculation. The absolute accuracy of the winds is ± 1 m s^{-1}; the relative accuracy is ± 0.1 m s^{-1}.

A measure of turbulence was obtained from a Meteorology Research, Incorporated turbulence meter model 11220 (MacCready 1964). This instrument measures dynamic pressure fluctuations using a Pitot tube. A filter limits the frequency response between 2 and 50 Hz, which corresponds to wavelengths of 2–50 m at an airspeed of 100 m s^{-1}. The output is an estimate of $\epsilon_0^{1/3}$, where ϵ_0 is the eddy dissipation rate, and ranges from 0 to 10 cm$^{2/3}$ s^{-1}.

Cloud hydrometeors were measured using four Particle Measuring Systems (PMS) probes: the forward-scattering spectrometer probe (FSSP) for diameters 3–45 μm, the 1D-C probe for diameters 12.5–187.5 μm, a 2D-C probe for diameters 25–800 μm, and a 2D-P probe for diameters 200–6400 μm.

Neither the FSSP nor the 1D-C records particle shape, thus, both ice particles and water droplets may be detected. The 2D probes provide two-dimensional images of particles that may be used to distinguish between ice and water. This information was used to infer what the 1D-C probe detected.

The 2D probes occasionally record so-called "zero-area" images. These are typically hydrometeors that are large enough to trigger the probe's recording devices but not large enough to completely shadow any of the photodiodes. Thus, they are probably of diameter 25 μm for the 2D-C probe, and 200 μm for the 2D-P probe. Zero-area images are often seen in the presence of large supercooled drops and in seeding plumes where large numbers of tiny ice crystals are present.

The FSSP may record counts in the presence of high ice crystal concentration as reported by Gardiner and Hallett (1985). However, for the present analysis, spectral contamination by ice crystals was not considered a problem; ice generally appears as low counts covering the entire size range of the probe. True droplet spectra are peaked and are, therefore, usually easy to distinguish from ice. FSSP-measured spectra were examined for this effect for the cases used in this study.

The Wyoming King Air is also equipped with a Johnson–Williams (JW) and a King liquid water measurement device. A Rosemount icing probe (model 871FA) was aboard as an additional check on icing conditions.

c. Definition of a large-drop region

Drops in the size range of interest, approximately thirty to several hundred micrometers in diameter, are particularly difficult to detect unambiguously using instrumentation typically mounted on current research aircraft. The 1D-C probe on the King Air measures the appropriate size range but does not give hydrometeor shape information; the 2D-C provides shape

but for sizes covering a few pixels ($\leqslant 150$ μm) particle type is difficult if not impossible to distinguish.

Based on past experience and measurements available for large-drop regions, we used the following criteria to define a large-drop region:

1) FSSP concentration greater than or equal to 5 cm^{-3} for drops with diameter greater than 22 μm,
2) 1D-C concentration greater than or equal to 5 L^{-1} for particles with diameter greater than 75 μm,
3) 2D-C concentration greater than or equal to 5 L^{-1} for zero-area images or distinguishable drops.

At least one of these criteria must be satisfied for classification as a large-drop region. The zero-area images criteria from the 2D-C probe was the most reliable detector of large-drop regions.

In moderate icing conditions, each of the PMS probes may experience ice accretion over the sampling orifice, restricting or totally obstructing the sample airflow. For this reason, redundancy was built into the definition of a large-drop region.

Additional checks were also made. The presence of ice was carefully considered, since all of the above conditions can be met by ice crystals rather than liquid droplets. The shape of the 2D images, the amount of liquid water measured by the King and JW probes, the shape of the FSSP spectrum, and the cycling rate of the Rosemount icing probe were examined when assessing the presence of large drops.

d. Definition of a dynamically unstable shear layer

The bulk Richardson number (Ri) was calculated across the shear layer as a measure of the wind shear–induced mixing and is defined as

$$\mathrm{Ri} = \frac{g}{\theta}\frac{\Delta\theta}{\Delta z}\left(\frac{\Delta \mathbf{V}}{\Delta z}\right)^{-2}, \qquad (1)$$

where g is the acceleration due to gravity, θ is potential temperature, $\Delta\theta$ and $\Delta\mathbf{V}$ are the changes in potential temperature and wind vector, respectively, across the shear layer Δz. The Richardson number is defined as the ratio of the work done against gravitational stability to kinetic energy transferred from mean to turbulent motion (as in Haurwitz 1941); Ri < 1.0 indicates that turbulence and KH waves are possible. It has been shown theoretically (Miles 1961; Howard 1961) that Ri = 0.25 is the critical value for the onset of turbulence and Ri < 1.0 is sufficient to maintain turbulence. This condition is referred to as dynamic instability (Stull 1988). Wind shear at the tops of clouds often results in billow clouds because moist stability ($\Delta\theta_m/\Delta z$) is much less than dry stability ($\Delta\theta/\Delta z$).

For the purposes of this research, a dynamically unstable shear layer (with the potential for causing turbulence and mixing) is assumed to exist when *all three* of the following conditions are present:

1) a distinct change in wind shear,
2) a shear value of at least 0.02 s^{-1},
3) a Ri < 1.0.

3. Results

a. General

Aircraft measurements from 29 soundings through cloud top are summarized in Table 1. All the clouds were stratiform. The split between stratus (St) and stratocumulus (Sc)[1] was 23 versus 6. The conditional instability ($\partial\theta_e/\partial z$) was negative above two of the St and four of the Sc cloud types.

The median depth of the shear layers (Δz) was 100 m, with a range of 20–400 m. In most cases the speed or directional shear was well defined (DEF in Table 1); however, in other cases the wind shear was more gradual or undefined (UND) in which case an arbitrary selection was made for the depth over which to calculate shear and Ri.

Turbulence usually peaked within the shear layer and at cloud top. The highest eddy dissipation rate ($\epsilon_0^{1/3}$) for each shear layer is listed in the table; most values would be classified as "moderate," a few "heavy," using the definitions of MacCready (1964).

The median cloud-top temperature of the cases studied here was −9.0°C, with a range of −5 to −16°C. These are slightly colder than the values listed by Politovich (1989); however, the Politovich temperatures were in-cloud temperatures and not necessarily cloud-top temperatures. Still, they are consistent with a temperature regime where high concentrations of ice crystals are not normally observed. An important difference between these results and those by Politovich is in droplet concentration (FSSP CONC); most of the cases in Politovich had values below 100 cm^{-3}, which led to the suggestion that a maritime droplet concentration was favored. Seven of the 19 cases in Table 1 with large-drop regions had droplet concentrations of at least 100 cm^{-3}.

Liquid water contents (LWC) are usually low, with a median value of 0.04 g m^{-3} and a maximum of 0.45 g m^{-3}. The 1D-C concentrations tend to be lower than the values cited by Politovich. The comments regarding 2D images reflect the uncertainty that can arise from particles in the lower end of the detected size range.

The median Ri was 0.51 with values ranging from 0.04 to 6.42. The storms flown during SCPP and WISP were primarily stable orographic clouds over the Sierra Nevada or shallow clouds associated with weak anticyclones in the Colorado Front Range of the Rocky Mountains. All the values of Ri were positive, reflecting the static stability above these stratiform clouds.

[1] We define St when the incloud θ_e increases with height and Sc when the incloud θ_e decreases with height.

b. Examples

The climb-out sounding for 13 February 1990 at 1723 UTC is presented in Fig. 1 and shows a 10°C inversion at cloud top (680 mb). Four soundings were obtained near cloud top to document the vertical structure of the top of the cloud (Table 1, cases 5–8). Two of these cloud-top soundings are discussed below.

At 1728 UTC (case 5), as the plane climbed above the stratiform cloud deck, the flight scientist noted "wave structures" at the cloud top that he estimated to be a few hundred meters in wavelength but with no evidence of breaking waves. Although the aircraft ascended and descended through this shear layer several times, no quantitative data to support the observed waves were recorded. The thickness of the shear layer was 110 m.

At 1739 UTC (case 6) the aircraft descended into cloud (Fig. 2). The droplet concentration was 7 cm^{-3} near cloud top. The concentration of droplets with $d \geq 22$ μm was 4 cm^{-3}, with the largest diameter being 30 μm. The 1D-C probe recorded concentrations of 35 L^{-1} with the concentration of particles with $d \geq 75$ μm being 5 L^{-1}. The 2D-C probe recorded high concentrations of zero-area images. The Rosemount icing probe cycled frequently indicating icing conditions, but the encounter lasted for only about 1 min. Degradation in aircraft performance was not mentioned on the voice tapes.

A distinct 150-m-deep shear layer is evident in Fig. 2. The wind in the cloud layer below 2900 m had an easterly or upslope component; above 2900 m the wind had a westerly component. The Ri in the shear layer was 0.17. The wind direction backed 31° and the speed

TABLE 1. Summary of data for case studies.

Event	Date	Time (UTC)	Δz (m)	DEF UND	$\epsilon_0^{1/3}$ ($cm^{2/3}$ s^{-1})	Ri	Shear (s^{-1})	Cloud-top temp (°C)	FSSP CONC Total/>22 μm (cm^{-3})	LWC (g m^{-3})	1D-C CONC Total/>75 μm (L^{-1})	2D Images	Stability Abv cld/ cld type	LDR/ DUL
1	12 Feb 1983	1552:36–1555:24	400	DEF	2.0	0.22	0.18	−6.2	6/0	0.00	800/200	zero areas sml circ	−/St	Y/Y
2		1559:18–1600:42	100	UND	5.0	0.11	0.06	−9.3	2/0	0.00	0/0	ice	−/St	N/N
3	1 Feb 1985	2243:00–2245:48	240	DEF	2.3	0.29	0.10	−12.0	17/7	0.05	0/0	zero areas	−/Sc	Y/Y
4		2303:48–2308:06	200	DEF	3.5	0.77	0.07	−13.0	5/1	0.03	30/5	ice, circ zero areas	+/St	Y/Y
5	13 Feb 1990	1726:30–1729:54	110	DEF	2.5	0.73	0.08	−16.0	4/2	0.12	35/5	zero areas	+/St	Y/Y
6		1738:00–1739:36	150	DEF	5.1	0.17	0.19	−9.0	7/4	0.07	15/4	zero areas	+/St	Y/Y
7		1858:36–1859:48	30	DEF	3.0	0.24	0.06	−12.0	6/2	0.09	35/2	zero areas	+/St	Y/Y
8		1915:30–1917:00	75	DEF	2.5	0.19	0.08	−10.0	40/3	0.07	15/1	zero areas	+/St	Y/Y
9	27 Feb 1990	1400:00–1401:42	60	DEF	2.8	0.17	0.09	−7.0	25/1	0.30	2/0	zero areas	+/St	Y/Y
10		1436:06–1436:42	40	DEF	2.2	0.24	0.02	−6.0	2/0	0.07	0/0	zero areas	+/St	Y/Y
11		1518:24–1520:00	120	DEF	2.2	1.55	0.02	−6.0	20/1	0.27	0/0	zero areas	+/St	Y/N
12		1534:18–1535:36	100	UND	2.6	0.47	0.03	−7.5	40/1	0.20	2/0	zero areas	+/St	Y/N
13	27 Feb 1990	2302:00–2303:54	150	UND	2.0	4.59	0.02	−10.0	110/30	0.45	0/0	ice	+/St	Y/N
14		2321:48–2322:24	20	UND	2.2	5.87	0.02	−11.0	50/10	0.40	450/15	zero areas drops	+/St	Y/N
15		2333:00–2333:54	100	UND	1.0	4.00	0.02	−9.0	200/6	0.45	100/6	zero areas ice	+/St	Y/N
16	2 Mar 1991	1518:54–1522:24	110	UND	1.0	0.04	0.04	−5.0	100/0	0.07	50/1	ice	+/St	N/N
17		1607:30–1612:12	50	DEF	2.0	0.19	0.06	−7.0	160/20	0.26	0/0	zero-areas sml circ	+/St	Y/Y
18	15 Mar 1991	1332:00–1334:30	180	UND	1.2	1.34	0.04	−8.0	360/0	0.10	0/0	no images	+/St	N/N
19		1421:54–1422:36	35	UND	1.6	0.94	0.01	−9.0	160/2	0.06	5/0	ice	+/St	N/N
20		1438:18–1440:18	22	DEF	3.4	0.22	0.04	−9.0	300/5	0.22	4/0	zero areas	+/St	Y/Y
21		1457:36–1458:18	35	UND	1.7	2.61	0.01	−6.0	350/0	0.13	15/0	ice	+/Sc	N/N
22		1527:12–1529:36	80	UND	1.5	0.51	0.03	−8.0	400/0	0.25	10/0	ice	+/St	N/N
23	1 Mar 1991	0111:06–0113:12	125	UND	<1.0	0.64	0.04	−6.0	160/0	0.01	0/0	ice	+/St	N/N
24		0158:12–0159:36	100	UND	<1.0	1.58	0.02	−8.0	300/2	0.20	15/0	ice	+/St	N/N
25		0302:30–0305:00	50	DEF	2.0	0.48	0.03	−6.0	250/12	0.33	15/0	zero areas	+/Sc	Y/Y
26		0311:48–1314:06	100	DEF	4.0	0.35	0.06	−5.0	400/1	0.30	40/6	zero areas	+/St	Y/Y
27	22 Mar 1991	0816:18–0819:30	100	UND	2.0	6.42	0.01	−9.7	450/0	0.17	0/0	ice	−/Sc	N/N
28		0833:12–0834:48	100	UND	3.0	0.31	0.02	−10.0	300/0	0.13	0/0	no images	−/Sc	N/N
29		1031:54–1034:00	100	UND	2.5	0.49	0.02	−11.0	250/7	0.30	15/0	ice	−/Sc	Y/N

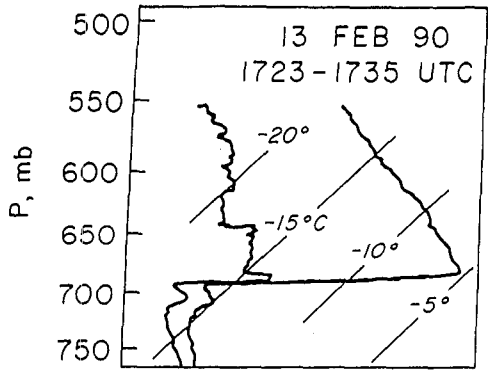

FIG. 1. Sounding of temperature and dewpoint on skew T-log$p$ diagram by Wyoming King Air during climb out from Jefferson County Airport on 13 February 1990 from 1723 to 1735 UTC.

increased from 8.5 to 22 m s^{-1}, providing a shear of 0.19 s^{-1}. The maximum eddy dissipation rate was 5.1 $cm^{2/3}$ s^{-1} near the bottom of the shear layer or top of the cloud where the moist static stability is less than the dry static stability. It should be noted that the turbulence was low in the cloud and above the shear layer.

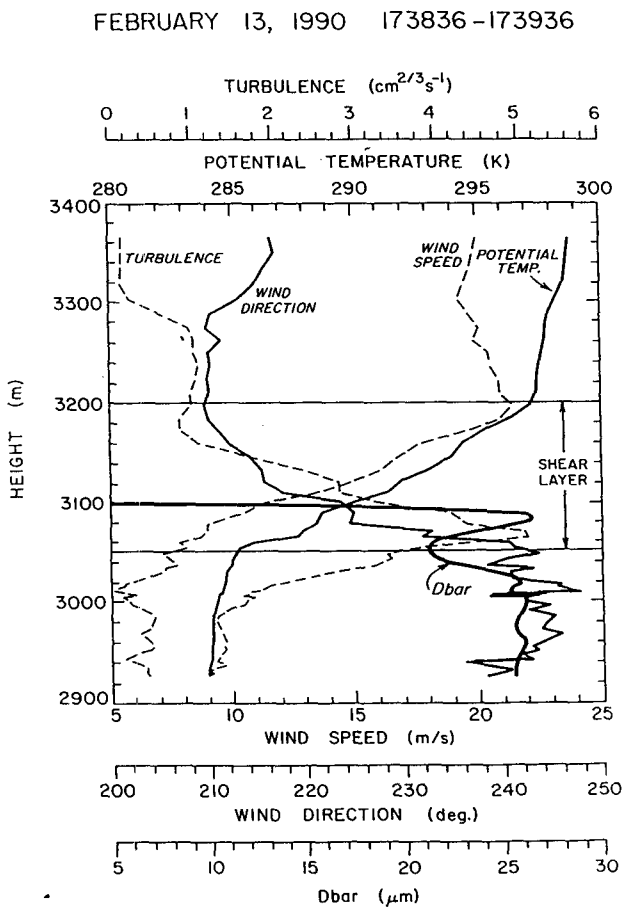

FIG. 2. Aircraft sounding for 1739 UTC 13 February 1990. Measurements of turbulence, potential temperature, wind speed, wind direction, and mean droplet diameter (Dbar) are shown. Shear layer is indicated by thin horizontal lines.

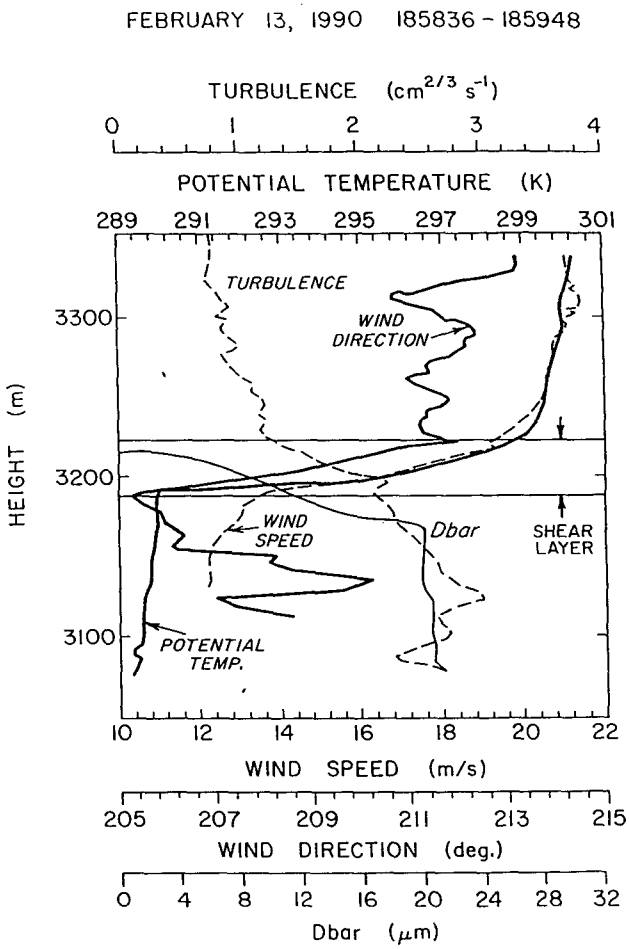

FIG. 3. Aircraft sounding for 1859 UTC 13 February 1990. Measurements of turbulence, potential temperature, wind speed, wind direction, and mean droplet diameter (Dbar) are shown. Shear layer is indicated by thin horizontal lines.

About an hour later, (case 7 at 1859 UTC, Fig. 3) while flying in the upper part of the cloud at 3050 m, severe icing was experienced for approximately 10 min. The icing was severe enough to cause noticeable degradation in aircraft performance, evidenced by the aircraft beginning to buffet. Upon climb out through the stratus cloud layer, the cloud top was at 3200 m and −12°C (Table 1). The FSSP-measured droplet concentration was still low at 6 cm^{-3}, with the concentration of droplets with $d \geq 22$ μm being 2 cm^{-3}. Mean droplet diameters from the FSSP were near 21 μm, with some droplets to 30 μm. The King device measured LWC values of 0.09 g m^{-3} near the cloud top and up to 0.41 g m^{-3} further into the cloud. The 2D-C recorded zero-area images, small circular images, and streakers until it stopped recording at about 1859 UTC. The streakers and stoppage of the 2D-C confirm the presence of rel-

atively high LWC for wintertime stratiform clouds. The Rosemount icing probe cycled continuously from 1855 to 1900 UTC, indicating icing and, as stated previously, the pilot noted that aircraft climb capability had deteriorated noticeably.

The Ri across the distinct 30-m-deep shear layer was 0.24. The wind direction veered 7° and the speed increased from 13.5 to 19 m s^{-1} across the layer, producing a shear value of 0.06 s^{-1}. The turbulence in the shear layer was less in this case than in the previous case but did extend at least 100 m down into the cloud layer. This suggests that a KH wave may have formed and collapsed, transferring turbulence from the shear layer down into the St cloud.

Although the aircraft performance degradation was most pronounced during this sounding, the mean droplet diameter measured by the FSSP was not the largest, nor the wind shear the strongest compared to the other three soundings obtained during this flight (see Table 1). It is possible that the aircraft performance degradation was a carryover effect from the previous icing encounter.

All four soundings on 13 February 1990 met the criteria for large-drop regions and dynamically unstable shear layers. There are slight variations: ice crystals were probably present in case 5 and case 8. Case 8 also had a slightly smaller mean droplet diameter and a higher droplet concentration. The droplet concentration was low in all cases, less than 40 cm^{-3}.

c. *Summary*

The relation of dynamically unstable shear layers to large-drop regions in stratiform clouds was evaluated using a contingency table (Table 2) based on the cases included in Table 1. Of the 29 cases considered, 13 had both large drops and dynamically unstable shear layers. Ten cases had neither. In six cases (11–15, 29) large drops were present without a dynamically unstable shear layer. Either there is yet another mechanism for producing large-drop regions, the sounding was not representative, or the mixing reduced the dynamic instability.

A χ^2 statistical test was applied to the contingency table data (Table 2) to test the hypothesis that dynamically unstable shear layers were related to large-drop regions. The null hypothesis was rejected at the 1% significance level. From this it can be inferred that dynamically unstable shear layers are associated with large-drop regions.

TABLE 2. Contingency table for case studies in Table 1.

		Dynamically unstable shear layer	
		Yes	No
Large droplets	Yes	1, 3, 4, 5, 6, 7, 8, 9, 10, 17, 20, 25, 26	11, 12, 13, 14, 15, 29
	No		2, 16, 18, 19, 21, 22, 23, 24, 27, 28, 29

4. Discussion

Dynamically unstable shear layers at cloud top may result in KH waves, the entrainment of subsaturated air, and turbulent mixing resulting in large-drop regions.

The cloud-top region typically consists of three distinct layers: the overlying unsaturated layer, the thin transition or shear layer, and the cloudy, saturated layer. The strongest turbulence ($\epsilon_0^{1/3}$) was observed within the dynamically unstable shear layer or in the top 100 m of the cloud layer. Both the overlying unsaturated layer and the saturated layer below were nonturbulent. *Mixing, therefore, appears to be a result of turbulence that develops in the shear or transition layer.* Since $\Delta\theta$ and ΔV are constant between the cloudy layer and the overlying unsaturated layer, an examination of Eq. (1) indicates that Ri decreases below 1.0 when Δz decreases either through ascent of the cloudy layer or descent of the overlying unsaturated layer.

The measurements needed to resolve the details of the mixing process(es) responsible for large drop formation are not available in the existing dataset. To provide direct evidence for the presence of KH waves within a dynamically unstable shear layer a careful examination of the aircraft data was made to locate an example of a KH wave at cloud top. In every case the aircraft ascended or descended rapidly through the shallow shear layers. We are, therefore, unable to provide direct evidence for the presence of KH waves and, hence, turbulent mixing in the tops of these clouds. Future research will concentrate on this objective.

The conditions previously suggested by Politovich (1989)—that is, low droplet concentration and warm cloud-top temperature—have generally been found to be present. A low droplet concentration, however, is not necessary, since several large-drop regions with high droplet concentrations were documented.

Forecasting large-drop regions presents a major challenge. The problem is confined to such thin shear layers that an accurate forecast that precisely pinpoints these regions is beyond the capability of current forecast models and observational technology. However, it may be possible to flag potential large-drop regions by examining wind shear in and above cloud along with thermodynamic and dynamic stability. Politovich (1989) discusses several synoptic situations that would favor the formation of large droplets: orographic, upslope, and warm-frontal situations. All these are consistent with the findings of this paper.

Acknowledgments. The cooperation of the King Air flight crew, particularly George Bershinsky and Glenn Gordon, was vital to the success of the large drop–seeking missions. Ben Bernstein aided in obtaining

some of the measurements. University of Wyoming authors were supported by NSF Grant ATM-9014763; NCAR funding was from Interagency Agreement DTFA0A-90-Z-02005 with the Federal Aviation Administration.

REFERENCES

Cooper, W. A., W. R. Sand, M. K. Politovich, and D. L. Veal, 1984: Effects of icing on performance of a research aircraft. *J. Aircraft,* **21,** 708–715.

Gardiner, B. A., and J. Hallett, 1985: Degradation of in-cloud forward scattering spectrometer probe measurements in the presence of ice particles. *J. Atmos. Oceanic Technol.,* **2,** 171–180.

Haurwitz, B., 1941: *Dynamic Meteorology.* McGraw-Hill, 365 pp.

Howard, L. N., 1961: Note on a paper by John W. Miles. *J. Fluid Mech.,* **10,** 509–512.

MacCready, P. B., 1964: Standardization of gustiness values from aircraft. *J. Appl. Meteor.,* **4,** 439–449.

Miles, J. W., 1961: On the stability of heterogeneous shear flow. *J. Fluid Mech.,* **10,** 496–508.

Politovich, M. K., 1989: Aircraft icing caused by large supercooled droplets. *J. Appl. Meteor.,* **28,** 856–868.

Rasmussen, R., M. Politovich, J. Marwitz, W. Sand, J. McGinley, J. Smart, R. Pielke, S. Rutledge, D. Wesley, G. Stossmeister, B. Bernstein, K. Elmore, N. Powell, E. Westwater, B. B. Stankov, and D. Burrows, 1992: Winter Icing and Storms Project (WISP). *Bull. Amer. Meteor. Soc.,* **73,** 951–974.

Reynolds, D. W., and A. S. Dennis, 1986: A review of the Sierra Cooperative Pilot Project. *Bull. Amer. Meteor. Soc.,* **67,** 513–523.

Sand, W. R., W. A. Cooper, M. K. Politovich, and D. L. Veal, 1984: Icing conditions encountered by a research aircraft. *J. Climate Appl. Meteor.,* **23,** 1427–1440.

Song, N., and J. D. Marwitz, 1989: A numerical study of the warm rain process in orographic clouds. *J. Atmos. Sci.,* **46,** 3479–3486.

Stull, R., 1988: *An Introduction to Boundary Layer Meteorology.* Kluwer Academic Publishers, 666 pp.